Investigation of mechanical properties of tubular aluminum foams

Article *in* International Journal of Materials Research (formerly Zeitschrift fuer Metallkunde) · September 2016

DOI: 10.3139/146.111430

CITATIONS
3

READS
237

5 authors, including:

Arif Uzun
Kastamonu Üniversitesi
17 PUBLICATIONS **31** CITATIONS
SEE PROFILE

Halil Karakoç
Hacettepe University
28 PUBLICATIONS **128** CITATIONS
SEE PROFILE

Ugur Gokmen
Gazi University
35 PUBLICATIONS **58** CITATIONS
SEE PROFILE

Investigation of mechanical properties of tubular aluminum foams

Article *in* International Journal of Materials Research (formerly Zeitschrift fuer Metallkunde) · September 2016

DOI: 10.3139/146.111430

5 authors, including:

Arif Uzun
Kastamonu Üniversitesi
14 PUBLICATIONS **10** CITATIONS
SEE PROFILE

Halil Karakoç
Hacettepe University
13 PUBLICATIONS **9** CITATIONS
SEE PROFILE

Mehmet Turker
Chalmers University of Technology
24 PUBLICATIONS **350** CITATIONS
SEE PROFILE

Arif Uzun[a], Halil Karakoc[b], Ugur Gokmen[c], Hanifi Cinici[d], Mehmet Turker[d]
[a] Department of Mechanical Engineering, Kastamonu University, Kastamonu, Turkey
[b] Ankara Chamber of Industry 1st Organized Industrial Zone Vocational School, Hacettepe University, Ankara, Turkey
[c] Technical Sciences Vocational School, Gazi University, Ankara, Turkey
[d] Department of Metallurgy and Materials Engineering, Gazi University, Ankara, Turkey

Investigation of mechanical properties of tubular aluminum foams

This manuscript focuses on the mechanical behavior under compressive and bending loadings of tubular aluminum foams. The tubular structures were manufactured using the powder metallurgy technique. Tubular aluminum foams were fabricated by heating foamable precursor materials above their melting temperature in a mould. The influence of important parameters such as wall thickness and density of foam on the mechanical properties was investigated. It was found that the 6 mm thick specimen showed a lower collapse strength than the thicker 9 mm specimen. Despite the decrease in densities of the samples, the collapse strength increased with the increase in wall thickness. The reduction of approximately 33 % in wall thickness (from $t = 9$ mm to 6 mm) decreased the bending performance of the tubular aluminum foams by approximately 50 %.

Keywords: Powder metallurgy; Cellular materials; Mechanical characterization; Al foam

1. Introduction

Metal foams have demonstrated improvements to many industrial applications due to their excellent physical and mechanical properties. Some of the features include great strength to density ratio excellent buckling behavior, vibration attenuation and great energy dissipation [1–3]. Today many industries can benefit from the advantages of metallic foams. For instance in the automotive industry weight reduction and energy dissipation capability can be achieved by increasing structure porosity. In contrast, the strength and stiffness of the structure may be reduced [4]. Hence, advanced analysis methods may be required to design metal foams for excellent physical and mechanical behavior in multifunctional applications [5]. Metallic foam production methods play a prominent role in the physical and mechanical characteristics of foams. The most efficient production methods used in the production of aluminum foam are the powder metallurgy (PM) technique [6] and the casting processes [1]. The powder metallurgy technique consist of heating a foamable precursor material, usually in a closed mold. The foamable material is produced by compressing the mixed metal powders (e. g. aluminum, copper, lead) and foaming agent (e. g. titanium hydride) using compaction techniques such as hot pressing, extrusion and rolling [7]. Finally, the production of foams with complex and simple shapes is carried out. Especially, the large and complex shaped foam parts could exhibit irregular pore size distribution and density gradient. This situation is the result of irregular bubble growth during the foam formation [8]. Aluminum (Al) foams have been widely used as an important material in aerospace, military equipment, automobiles, railways and other industries due to their excellent performance in strength per weight and high-performance energy absorption capacity [9, 10].

It is well known that mechanical behavior of closed-cell Al foams depends on relative density and macro-structural features such as pore size, pore structure and cell wall thickness. Recently, there have been many studies to understand structure–property relationships. Generally, elastic and plastic deformations in the aluminum foam are not uniform [11]. The mechanical property reflections of cellular metals are associated with bending and stress [1]. Cellular structures that are exposed to high amounts of local stresses have low yield strength. In contrast, the strain in the cell walls without bending makes the system rigid and resistant [12]. In particular, closed-cell Al foams can absorb higher levels of energy than dense Al [7]. Al foams exhibit elastic behavior initially during compressive loading and then the plateau region occurs with plastic deformation. This region continues until the beginning of densification of the foam, and this reflects an important feature of its energy absorbing behavior [7, 13]. Most studies have been conducted to determine the mechanical behavior of metallic foams, especially on plateau stress, compressive strength, bending strength and Young's modulus [14–18]. Compressive strength and elastic properties of Al foams produced by the powder metallurgy (PM) method increase with increase of density [19]. For the deformation behavior of different types of Al foams (Alulight, Alporas), the inhomogeneity density distribution is a key factor [20]. In addition, it is reported that the sample size has a significant effect on the plastic collapse stress and elastic modulus of cellular material [21]. However, some researchers indicated that the bending strength of Al foam increases with increasing relative density [18, 22]. In these studies, mostly square or circular solid Al foams were tested. In the literature, there are no studies on the determination of mechanical properties of tubular Al foams. However, studies on the foam-filled metal tube (tubular) rather than a tubular foam can be found. The majority of these scientific studies have been published on the mechanical behavior of empty and foam-filled thin-walled structures with different circular cross-

sectional areas under axial compressive loading [7, 23–28]. Thin walled structures made with Al-alloys have been widely used to create important components in areas such as automobile, railway, aerospace industries [29]. In the future, tubular Al foams may be used instead of these materials.

In this paper, tubular Al foams with three different cross-sections were prepared based on the PM technique by heating the foamable precursor material inside a steel mold. The influence of important parameters such as wall thickness and density of foam on the mechanical behavior under compressive and bending loadings was investigated.

2. Experimental procedure

2.1. Raw materials and foamable precursor preparation

In the experiments, air atomized Al powder (ECKA Granules) with particle size <160 μm and elemental Si powder (Atlantic Equipment Engineers) with particle size <10 μm were used as the starting materials. TiH_2 (<44 μm, Sigma-Aldrich) was chosen as the foaming agent.

The production of foamble precursor consisted of five steps: (1) mixing: Al, Si powders (7 wt.%) with foaming agent (1 wt.%) were blended by a three-dimensional mixer for 30 min. (2) Cold pressing: the mixture powders were compacted as unidirectional at the room temperature under 400 MPa in a steel die to prepare semi-finished cylindrical specimens with size of 62 mm in diameter and 80 mm in thickness (Fig. 1a). (3) Sintering treatment: the semi-finished cylindrical specimens were pre-sintered to achieve a more intense structure and to facilitate extrusion at a temperature of 550 °C for 60 min. (4) Extrusion: the samples after sintering treatment were extruded (extrusion rate = 1 : 4) at 550 °C in order to produce foamable precursor samples with a 25×30 mm^2 cross-sectional area (Fig. 1b). (5) Rolling process: after extrusion the samples were rolled to obtain a plate thickness of 5 mm. This process was carried out in 5 cycles (Fig. 1c). Figure 2 illustrates the production process of foamable precursor material schematically.

2.2. Production of tubular Al foams

In the present study, tubular Al foams having 30 mm in diameter and 100 mm in length were prepared using the powder metallurgy (PM) method. The foamable precursor was inserted in a cylindrical steel mold with diameter of 34 mm and length of 110 mm. This mold is composed of five parts (Fig. 3). There are holes on the upper part (number 2) of the foaming mold. These holes are very important for the completion of the foaming process, because the process control was carried out through these holes. The mold was put in a resistance furnace which had been preheated to a temperature of 750 °C. The precursor started to foam after it was heated for a certain time. Subsequently, it took the shape of the mold and then ejected through holes on the upper part of the foaming mold. At this moment the mold was taken out of the furnace and cooled in air, and finally the tubular Al foams with different cross-sections were obtained. The samples have external and internal dense metal thin skins. These dense skins give a good surface finish to the specimens, as well as improving mechanical behavior [30]. Figure 4 shows tubular Al foams with different cross-sections.

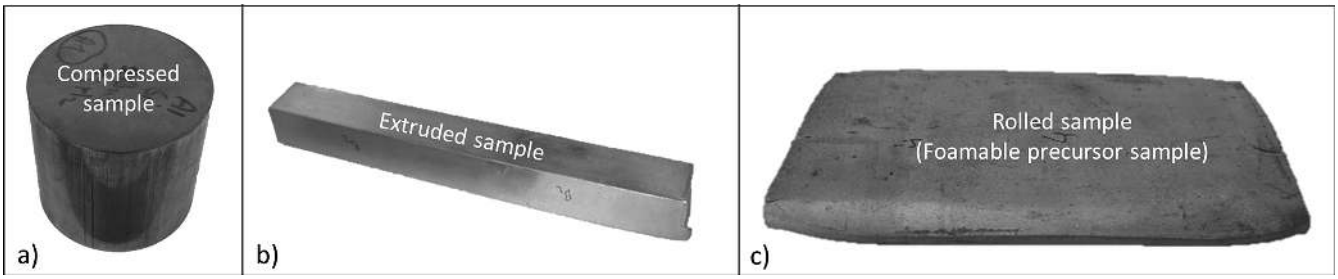

Fig. 1. (a) Compressed sample (∅ 62 × 80 mm), (b) Extruded sample (25×30 mm^2 cross-section), (c) Foamable precursor sample (thickness: 5 mm, width: 60–90 mm, length: 120–150 mm).

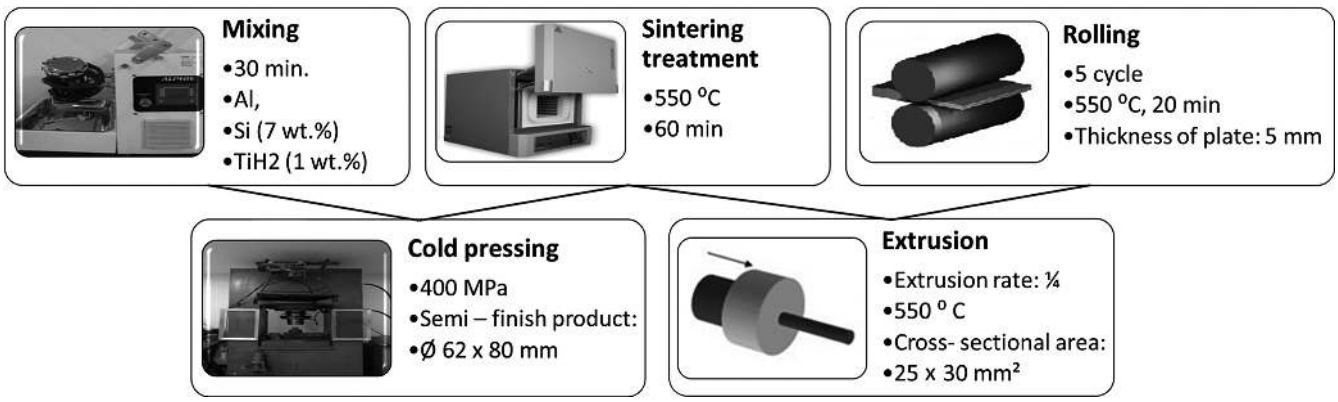

Fig. 2. Production process of foamable precursor material.

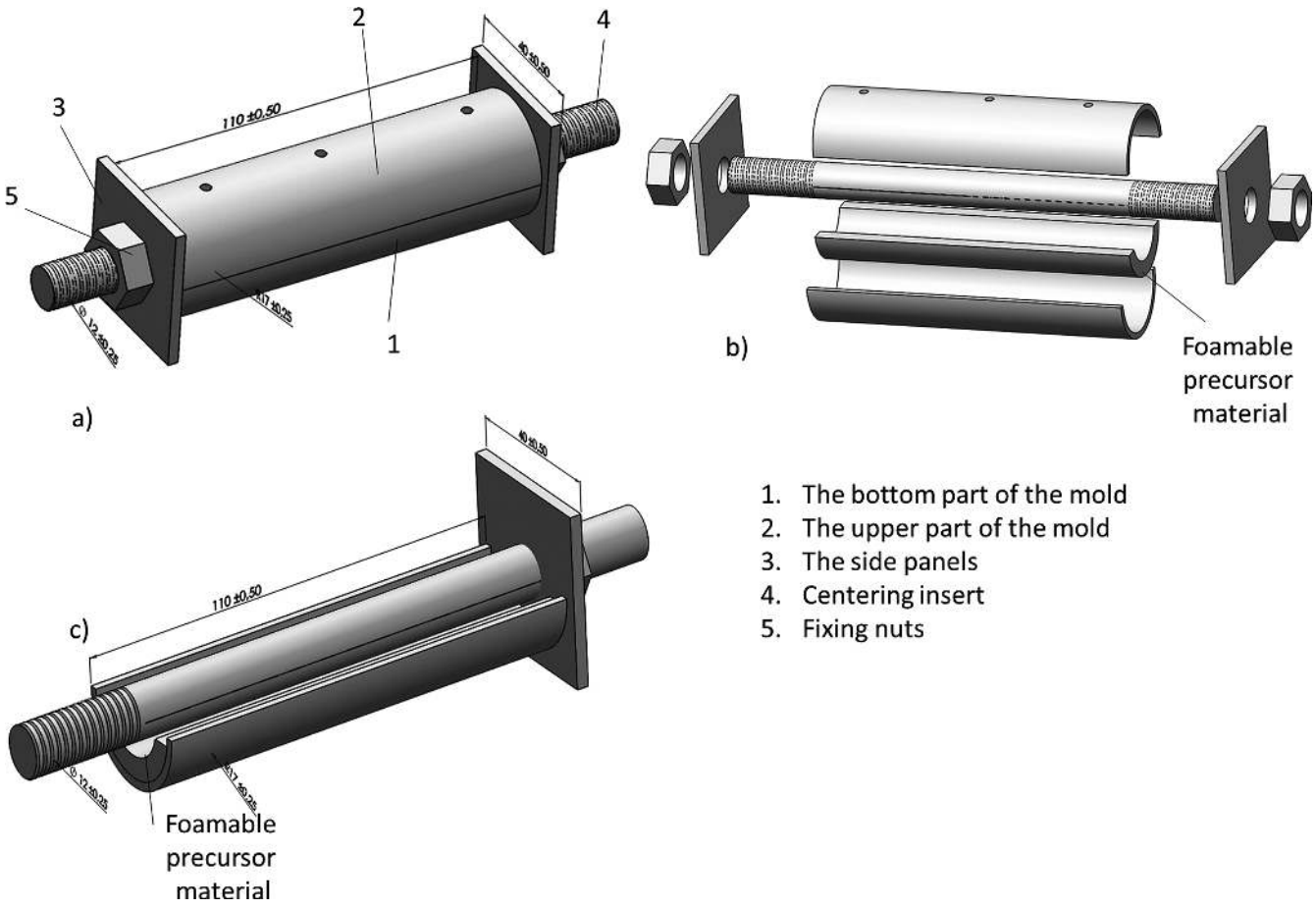

Fig. 3. (a) Foaming mold (assembly drawing), (b) foaming mold parts, (c) position of foamable precursor material in mold.

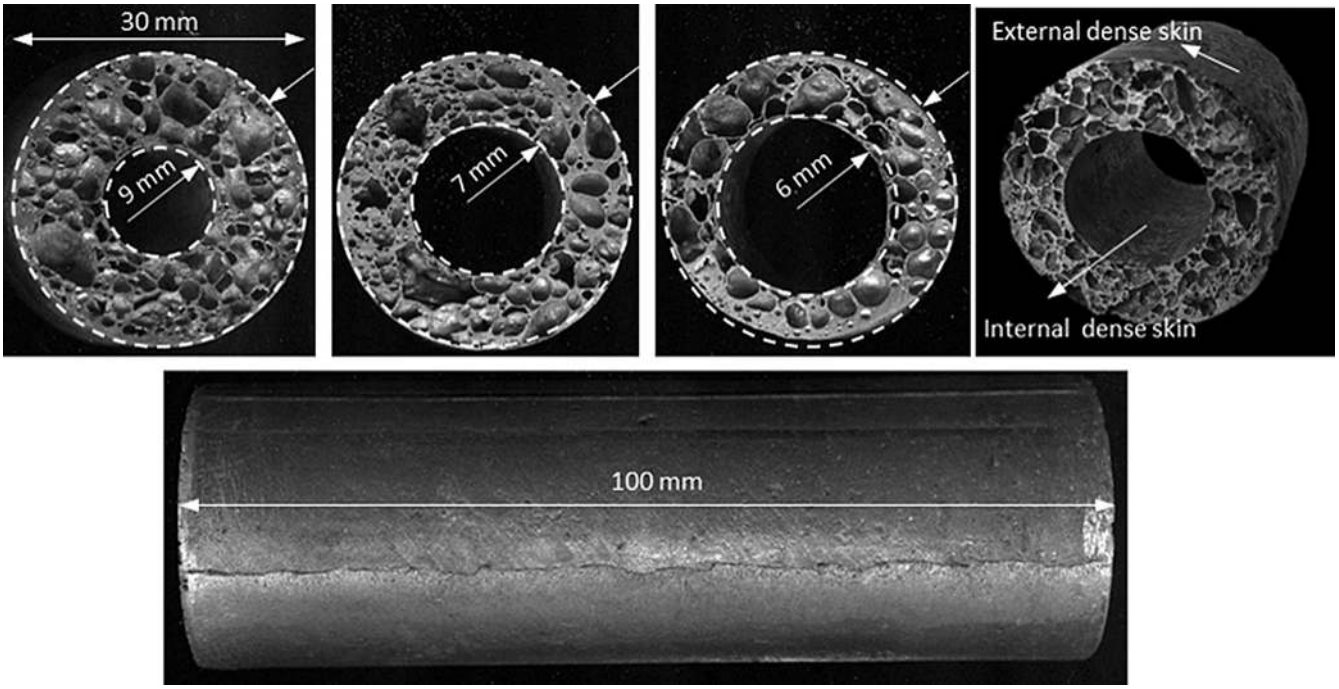

Fig. 4. Tubular Al foams with different cross-sections.

2.3. Compression testing

Using the fabricated foams, cylindrical tubular compression specimens having a constant external diameter (∅ 30 mm) and different internal diameters (∅ 12, 16 and 18 mm) were cut to a length of 30 mm by electro-discharging machine. Quasi-static compression tests were carried out at room temperature on a universal testing machine (Instron 3369) with a constant cross-head speed of 1 mm min^{-1}, and the stress (σ)–strain (ε) curves were recorded using a computer. Three typical Al foam samples (length 30 mm) as shown in Fig. 5 were tested and three specimens of each type of the tubular foam studied in this work were used.

2.4. Bending tests

The tubular Al foam samples were subjected to three-point bending tests under quasi-static loading conditions using a universal testing machine (Instron 3369). The cross-head speed was 1 mm min^{-1}. The specimen was placed on two cylindrical supports (*R:5* mm, 60 mm support distance) and bended by middle cylinder (*R:5* mm), as shown in Fig. 6. The cylinder tubular compression specimens having a constant external diameter (∅ 30 mm) and different internal diameter (∅ 12, 16 and 18 mm) were cut to the length of 100 mm by electric cutting machine for the bending tests. Three specimens of each type of the foams studied in this work were tested.

3. Results and discussion

3.1. Compressive behavior

The load–displacement curves were used to calculate the stress–strain curves. Some calculated curves for tubular Al foams with different cross-sections are shown in Fig. 7. The variations in the load–displacement curves led to differences in the compressive strength. This situation was due to the sample thickness, density and internal defects [31]. The average density of the samples was measured to be 0.80 g cm^{-3} for t = 6 mm, 0.71 g cm^{-3} for t = 7 mm and 0.68 g cm^{-3} for t = 9 mm. This difference in density occurred because of the precursor samples, which have the same volume. So, the thicker-walled samples (t = 9 mm) are expanded more than the other samples. Therefore, the cell size and shape of the sample is changed. The effects of missing cells or fractured cells on the compressive properties have been well presented in the studies by Chen et al. [32, 33]. The stress–strain curves were differentiated. The t = 6 mm specimen showed lower collapse strength than the thicker t = 9 mm specimen. First, the stress–strain curve increases linearly up to a certain value of the compressive

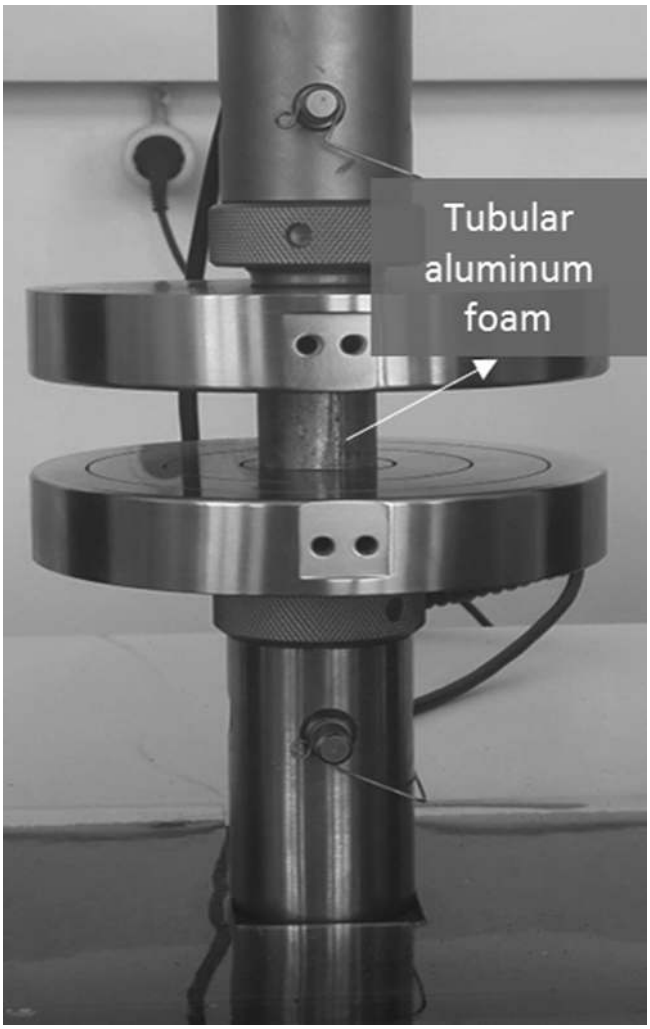

Fig. 5. Compression test.

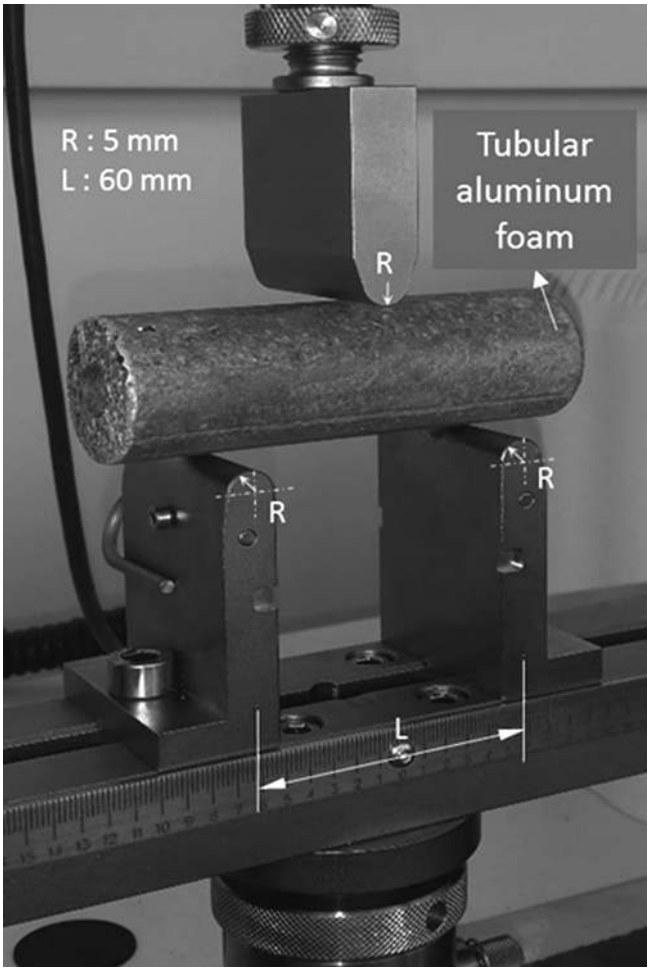

Fig. 6. Three-point bending test.

strain. The collapse strength υ^*_{pl} of the specimens varies from an average of 10 to 17 MPa (Fig. 7).

As shown in Fig. 8, the deformation modes of metal foams are classified into three types: (I) plastic bending of cell walls and edges, (II) elastic/plastic buckling and cell collapse and (III) tearing and breaking. In the stress–strain curves, the buckling and tearing failure are more pronounced compared with the bending deformation mode [34] because they lead to a significant reduction of stress. It is seen that all of the tubular foams were axisymmetrically crushed during deformation. However, the crushing mode may change for foam samples having other diameters and wall thicknesses. In particular, the ratio of diameter to thickness (d/t) is very important for the crushing behavior for circular thin-walled tubes [24].

One of the important objectives of this study was to determine the effects of the wall thickness on the collapse strength. Figure 9a shows the dependence of υ^*_{pl} on the wall thickness for tubular Al foams having the same outside diameter. In addition, the collapse strength is divided by the density of foam to normalize the results (Fig. 9b) because the specimens have different densities. Despite the decrease in densities of the samples, collapse strength increased with increase in wall thickness. Normally, strength increases with increase in density [35]. This is a usual effect of the foam density on the mechanical properties reported in [7, 35].

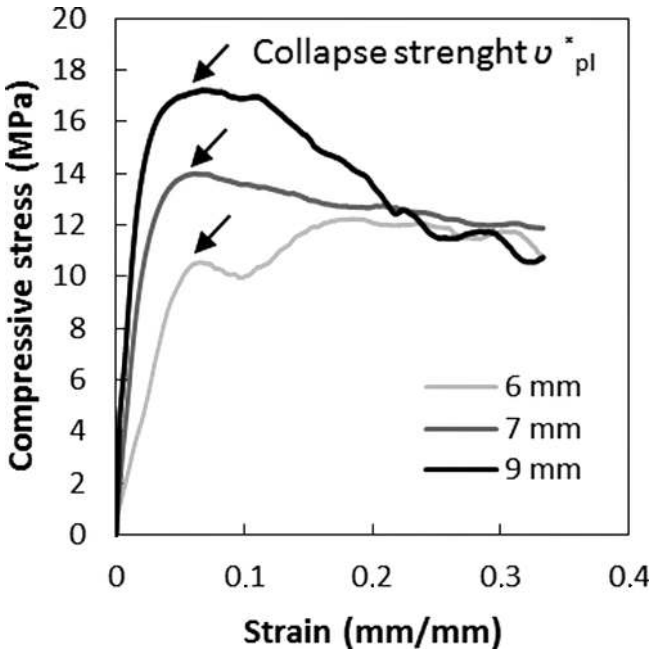

Fig. 7. Compressive stress–strain curves of tubular Al foams with different cross-section, t = wall thickness. Note: the specimens have different densities.

3.2. Bending behavior

The load–deflection curves under bending loading conditions of tubular Al foams with different cross-sections are shown in Fig. 10. There are clearly visible differences in the shapes of these curves, depending on the wall thickness

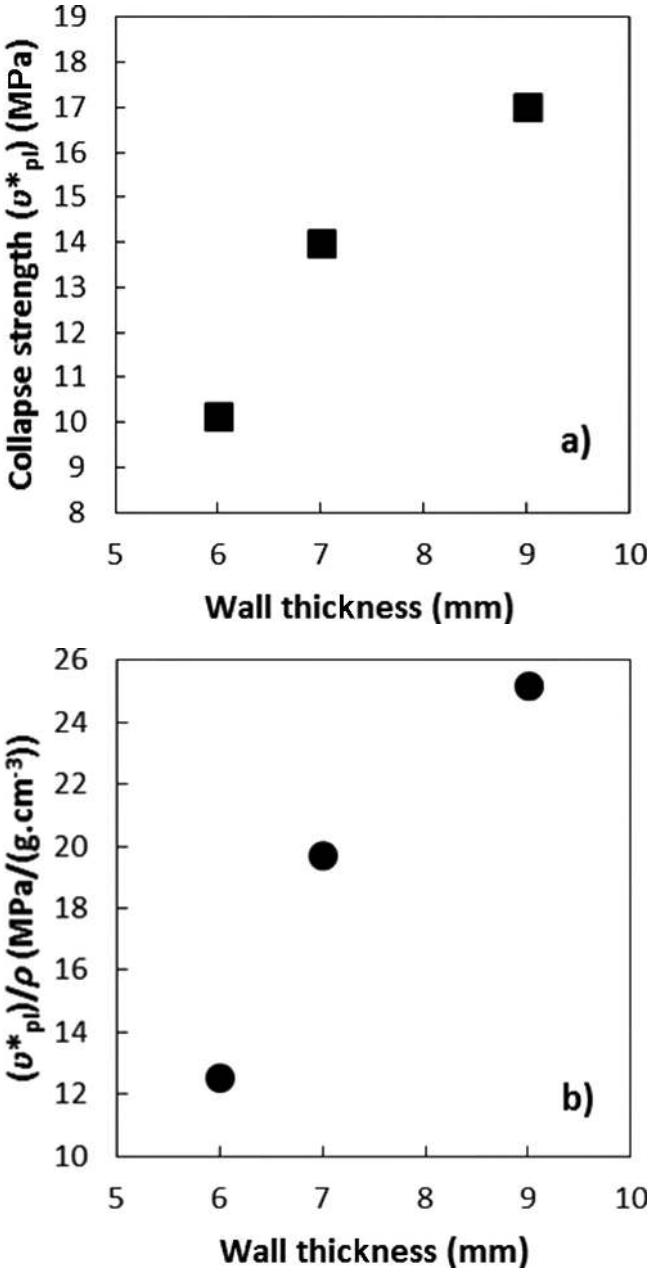

Fig. 9. (a) Collapse strength υ^*_{pl} vs wall thickness of tubular Al foams, and linear trend lines showing a strong dependence of υ^*_{pl} on the wall thickness, (b) Normalized collapse strength υ^*_{pl}/ρ vs wall thickness.

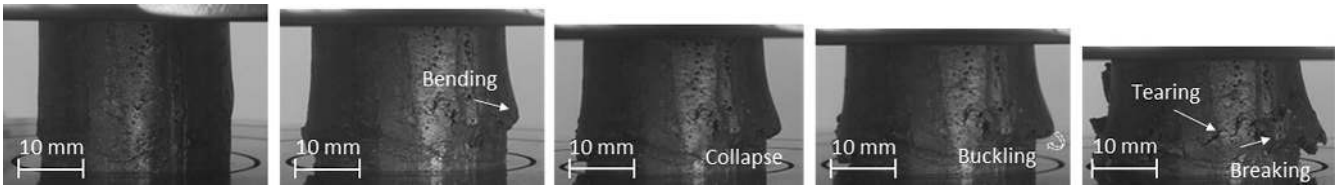

Fig. 8. Deformation sequence of tubular Al foam (t = 9 mm) subjected to uniaxial compression.

of the tubular foams. This depends on the section thickness of the cellular structure rather than the density of the foams. This action may be due to the differences in moment of inertia. The change in the properties of the tubular foams is due to the difficulty in controlling and adjusting the cellular structure during the manufacturing process [7, 36]. Despite the decrease in densities of the samples, bending strength increased with the increase in wall thickness. As previously mentioned, the strength increases with increase in density. However, this is the usual effect of foam density on the mechanical properties for tubular foams [22, 37, 38]. Foam samples exhibited elastoplastic deformation behavior until crack initiation as Al-alloy cylindrical foams [13]. The load rapidly dropped after reaching the maximum value and finally results in the specimen's failure [39]. The cracks started in the middle of all samples, which is the maximum tension region. The reduction of approximately 33 % in wall thickness (from 9 mm to 6 mm) decreased the bending performance of the tubular Al foams by approximately 50 %. The maximum achieved load levels are as follows: ~1.8 kN (t = 6 mm), ~2.8 kN (t = 7 mm) and ~3.5 kN (t = 9 mm).

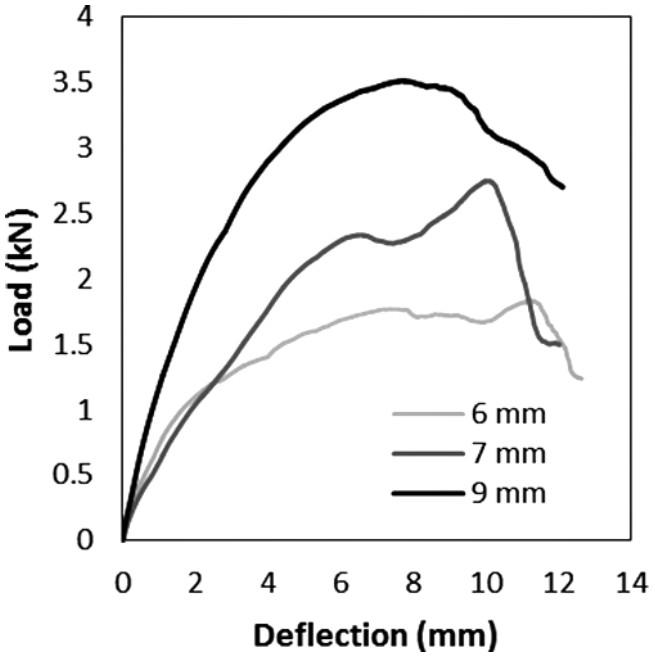

Fig. 10. The load–deflection curves under bending loading conditions for tubular Al foams.

The deformation and failure modes of three typical tubular Al foam samples during the bending loading process are shown in Fig. 11. The formation of cracks in all samples can be seen from these images. Tubular foams cracked with a brittle fracture mechanism in the middle under the loading point where the formation of tension stresses occurs. In this point, deformation bands do not occur as were formed during compression because buckling caused by tension is different from buckling caused by compression [13]. The cell edges are stretched rather than buckled. This behavior is observed in three-point bending tests of foams. The formation of cracks occurs rapidly and leads to a rapid load drop. It is thought that cell walls and cell edges crack before crack propagation in the outer surface starts [7, 13]. In addition, indentation was observed in the region of contact for all three cylindrical supports. This indention depth is one of the important differences observed in the deformation of tubular structures [13].

3.3. Energy absorption property

The energy absorption (EA) of tubular Al foam samples was evaluated from the integral of the area under the load–deflection curve. This value was calculated by the formula

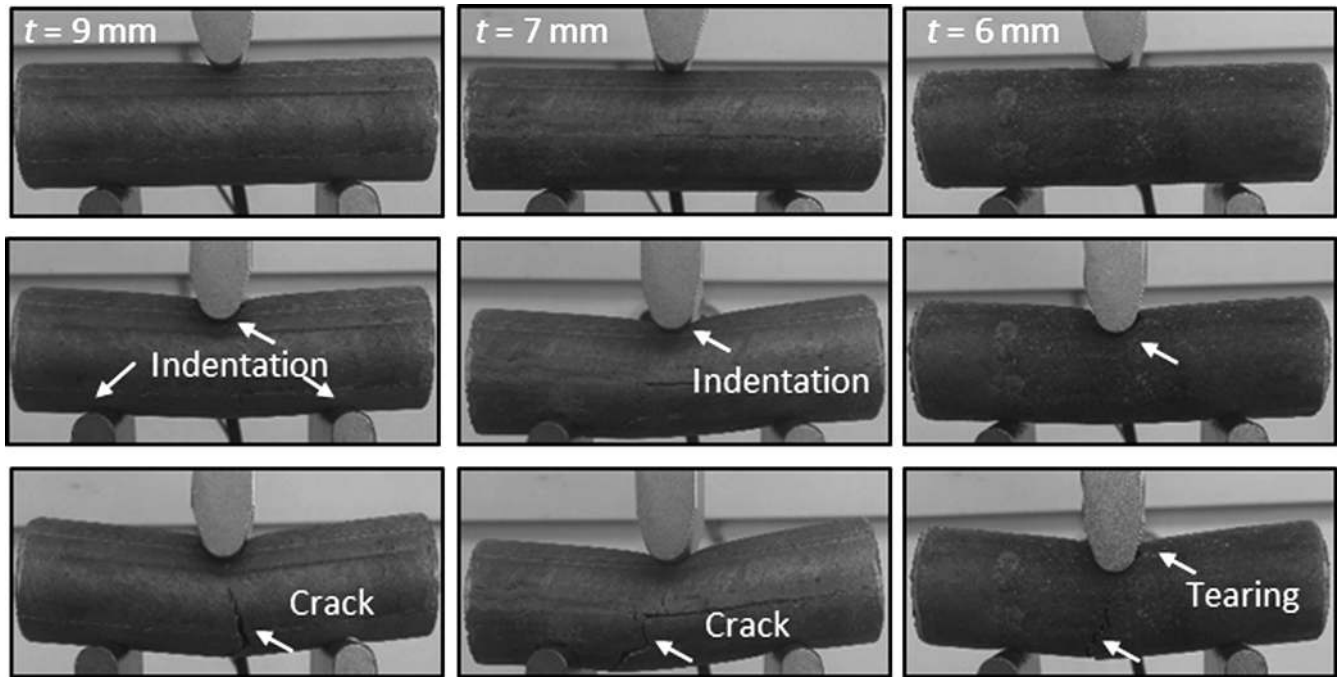

Fig. 11. Deformation sequence of three typical tubular Al foam samples during the bending loading conditions.

given in Eq. (1), where $F(\delta)$ is the instantaneous bending force as a function of the displacement δ [40].

$$EA = \int_0^{\delta} F(\delta)\mathrm{d}\delta \tag{1}$$

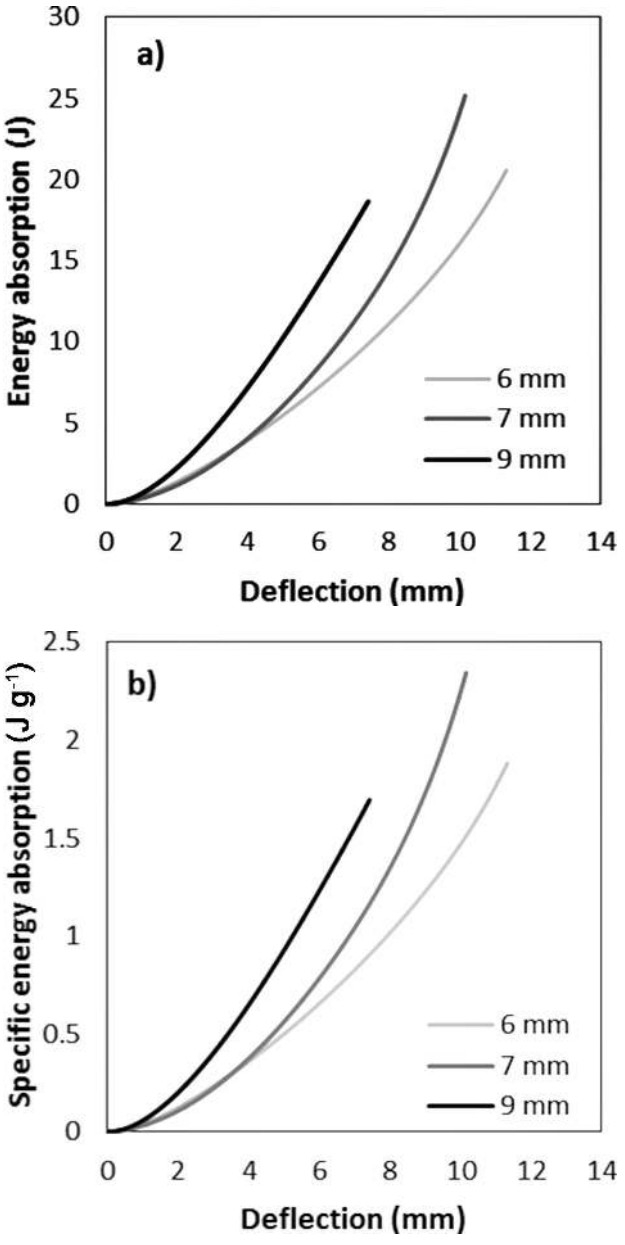

Fig. 12. (a) *EA*, and (b) *SEA* of the tubular foams under three-point bending loading.

The specific energy absorption (*SEA*) was calculated by the formula given in Eq. (2), where (EA_{total}) is the absorbed energy and M_{total} is the structure's total mass.

$$SEA = \frac{EA_{\text{total}}}{M_{\text{total}}} \tag{2}$$

EA and *SEA* diagrams for tubular foams are shown in Fig. 12. In addition, the values of the *EA* and *SEA* of tubular foams measured at the maximum load value are listed in Table 1. The values of the peak load for 9 and 7 mm thick tubular foams with different densities are approximately 1.92 and 1.50 times higher than for 6 mm thick tubular foam. However, it is difficult to say the same thing for *EA* and *SEA* maximum values because the deflection was shortened despite the increase in load. The 7 mm thick tubular foams tend to absorb more energy, but fail at lower deflection (see Fig. 12).

The changes in *EA* and *SEA* calculated at different deflections are given in Tables 2 and 3, respectively. The *EA* and *SEA* values of tubular foams depend on wall thickness, increasing up to 7 mm by the increase in thickness. At this deflection, the *EA* and *SEA* values of 9 mm thick tubular foam are about 89 % and 87 % higher than for 6 mm thick tubular foam, respectively.

4. Conclusions

The mechanical behavior under compressive and bending loadings of tubular Al foams was investigated. The effects of important parameters such as wall thickness and density of tubular foams on mechanical properties were studied. Some important results are the following:

- The $t = 6$ mm specimen showed lower collapse strength than the thicker $t = 9$ mm specimen. The average collapse strengths υ^*_{pl} of the 6, 7 and 9 mm thick specimens are 10 MPa, 14 MPa and 17 MPa, respectively.
- Despite the decrease in densities of the sample, bending strength increased with the increase in wall thickness. The reduction of approximately 33 % in wall thickness (from $t = 9$ mm to 6 mm) decreased the bending performance of the tubular Al foams by approximately 50 %. The maximum achieved load levels are as follows: ~1.8 kN ($t = 6$ mm), ~2.8 kN ($t = 7$ mm) and ~3.5 kN ($t = 9$ mm).
- Tubular foams cracked with a brittle fracture mechanism in the middle under the bending loading point where the tension stresses are formed because buckling caused by tension is different from buckling caused by compression.

Table 1. Maximum load values of tubular foams.

Wall thickness (mm)	Foam mass (g)	Foam density (g cm^{-3})	Peak			
			Load (kN)	Deflection (mm)	*EA* (J)	*SEA* (J g^{-1})
6	10.93	0.80	1.83	11.27	20.30	1.85
7	10.73	0.71	2.70	10.09	24.67	2.30
9	11.00	0.65	3.52	7.69	19.67	1.79

Table 2. Changes in *EA* at different deflections.

Wall thickness (mm)	Foam mass (g)	Foam density (g cm^{-3})	Deflection (mm)					
			7	5	3	7	5	3
			EA (J)			Changes in *EA* depends on the wall thickness (%)		
6	10.93	0.80	9.04	5.46	2.55	–	–	–
7	10.73	0.71	11.16	6.03	2.39	23.45	10.44	– 6.27
9	11.00	0.65	17.08	10.20	4.43	88.94	86.81	73.73

Table 3. Changes in *SEA* at different deflections.

Wall thickness (mm)	Foam mass (g)	Foam density (g cm^{-3})	Deflection (mm)					
			7	5	3	7	5	3
			SEA (J)			Changes in *SEA* depends on the wall thickness (%)		
6	10.93	0.80	0.83	0.50	0.23	–	–	–
7	10.73	0.71	1.04	0.56	0.22	25.30	12.00	– 4.35
9	11.00	0.65	1.55	0.92	0.40	86.75	84.00	73.91

- The *EA* and *SEA* values of tubular foams depend on wall thickness and increased with increase in thickness up to 7 mm.

References

[1] J. Banhart: Prog. Mater. Sci. 46 (2001) 559. DOI:10.1016/S00796425(00)00002-5
[2] R. Neugebauer, T. Hipke: Adv. Eng. Mater. 8 (2006) 858. DOI:10.1002/adem.200600095
[3] H. Bafti, A. Habibolahzadeh: Mater. Des. 52 (2013) 404. DOI:10.1016/j.matdes.2013.05.043
[4] P. Pinto, N. Peixinho, F. Silva, D. Soares: J. Mater. Process. Technol. 214 (2014) 571. DOI:10.1016/j.jmatprotec.2013.11.011
[5] J. Kadkhodapour, H. Montazerian, M. Samadi, S. Schmauder, A. Abouei Mehrizi: Mater. Des. 83 (2015) 352. DOI:10.1016/j.matdes.2015.05.086
[6] F. Baumgärtner, I. Duarte, J. Banhart: Adv. Eng. Mater. 4 (2000) 168. DOI:10.1002/(SICI)1527-2648(200004)2:4<168::AID-ADEM168>3.0.CO;2-O
[7] H.P. Degischer, B. Kriszt: Handbook of cellular metals: production, processing, applications, Wiley-VCH Verlag GmbH, Weinheim (2002). DOI:10.1002/3527600558
[8] I. Duarte, J. Banhart: Acta Mater. 48 (2000) 2349. DOI:10.1016/S1359-6454(00)00020-3
[9] W. Abramowicz, N. Jones: Int. J. Impact Eng. 4 (1986) 243. (86)90017–5. DOI:10.1016/0734-743X
[10] E. Ghassemieh, in: C. Marcello, (Ed.), New trends and developments in automotive industry, In Tech, Rijeka (2011) 365.
[11] M. Saadatfar, M. Mukherjee, M. Madadi, G.E. Schroder-Turk, F. Garcia-Moreno, F.M. Schaller, S. Hutzler, A.P. Sheppard, J. Banhart, U. Ramamurty: Acta Mater. 60 (2012) 3604. DOI:10.1016/j.actamat.2012.02.029
[12] A.G. Evans, J.W. Hutchinson, M.F. Ashby: Prog. Mater. Sci. 43 (1999) 171. DOI:10.1016/S0079-6425(98)00004-8
[13] I. Duarte, M. Vesenjak, L.K. Opara: Compos. Struct. 109 (2014) 48. DOI:10.1016/j.compstruct.2013.10.040
[14] E. Andrews, W. Sanders, L.J. Gibson: Mater. Sci. Eng. A-Struct. 270 (1999) 113. DOI:10.1016/S0921-5093(99)00170-7
[15] D.P. Mondal, N. Ramakrishnan, K.S. Suresh, S. Das: Scr. Mater. 57 (2007) 929. DOI:10.1016/j.scriptamat.2007.07.021
[16] D.P. Mondal, M.D. Goel, S. Das: Mater. Sci. Eng. A-Struct. 507 (2009) 102. DOI:10.1016/j.msea.2009.01.019
[17] C. Motz, R. Pippan: Acta Mater. 49 (2001) 2463. DOI:10.1016/S1359-6454(01)00152-5
[18] A. Uzun, M. Turker: Int. J. Mater. Res. 106 (2015) 970. DOI:10.3139/146.111257
[19] E. Koza, M. Leonowicz, S. Wojciechowski, F. Simancik: Mater. Lett. 58 (2003) 132. DOI:10.1016/S0167-577X(03)00430-0
[20] B. Kriszt, B. Foroughi, K. Faure, H.P. Degischer: Mater. Sci. Technol. 16 (2000) 792. DOI:10.1179/026708300101508450
[21] I. Jeon, T. Asahina: Acta Mater. 53 (2005) 3415. DOI:10.1016/j.actamat.2005.04.010
[22] M. Malekjafarian, S.K. Sadrnezhaad: Mater. Des. 42 (2012) 8. DOI:10.1016/j.matdes.2012.05.036
[23] M. Guden, H. Kavi: Thin Walled Struct. 44 (2006) 739. DOI:10.1016/j.tws.2006.07.003
[24] Z. Li, J. Yu, L. Guo: Int. J. Mech. Sci. 54 (2012) 48. DOI:10.1016/j.ijmecsci.2011.09.006
[25] L. Mirfendereski, M. Salimi, S. Ziaei-Rad: Int. J. Mech. Sci. 50 (2008) 1042. DOI:10.1016/j.ijmecsci.2008.02.007
[26] H.R. Zarei, M. Kroger: Int. J. Impact Eng. 35 (2008) 521. DOI:10.1016/j.ijimpeng.2007.05.003
[27] W. Abramowicz, T. Wierzbicki: Int. J. Mech. Sci. 30 (1988) 263. DOI:10.1016/0020-7403(88)90059-8
[28] M. Seitzberger, F.G. Rammerstorfer, H.P. Degischer: Acta Mech. 125 (1997) 93. DOI:10.1007/BF01177301
[29] W. Abramowick: Thin Walled Struct. 41 (2003) 91. DOI:10.1016/S0263-8231(02)00082-4
[30] I. Duarte, M. Oliveira, in: K. Kondoh (Ed.), Aluminium alloy foams: production and properties, In Tech, Rijeka (2012) 47.
[31] U. Ramamurty, A. Paul: Acta Mater. 52 (2004) 869. DOI:10.1016/j.actamat.2003.10.021
[32] C. Chen, T.J. Lu, N.A. Fleck: J. Mech. Phys. Solids 47 (1999) 2235. DOI:10.1016/S0022-5096(99)00030-7
[33] C. Chen, T.J. Lu, N.A. Fleck: Int. J. Mech. Sci. 43 (2001) 487. DOI:10.1016/S0020-7403(99)00122-8
[34] P. Wang, S. Xu, Z. Li, J. Yang, H. Zheng, S. Hu: Mater. Sci. Eng. A-Struct. 599 (2014) 174. DOI:10.1016/j.msea.2014.01.076
[35] I. Duarte, M. Vesenjak, L. Krstulović-Opara: Mater. Sci. Eng. A-Struct. 616 (2014) 171. DOI:10.1016/j.msea.2014.08.002
[36] M. Mukherjee, U. Ramamurty, F. Garcia-Moreno, J. Banhart: Acta Mater. 58 (2010) 5031. DOI:10.1016/j.actamat.2010.05.039

[37] S. Santos, T. Wierzbicki: Int. J. Mech. Sci. 41 (1999) 995. DOI:10.1016/S0020-7403(98)00066-6
[38] I. Duarte, M. Vesenjak, L.K. Opara, I. Anzel, M.F. Ferreira José: Mater. Des. 66 (2015) 532. DOI:10.1016/j.matdes.2014.04.082
[39] G.B. Broggiato, F. Campana, L. Peroni, in: J. Banhart, N.A. Fleck, A. Mortensen, (Eds.), Cellular metals: manufacture, properties and applications, MIT-Verlag, Berlin (2003) 445.
[40] T. Mukai, H. Kanahashi, T. Miyoshi: Scr. Mater. 40 (1999) 921. DOI:10.1016/S1359-6462(99)00038-X

(Received June 11, 2016; accepted August 2, 2016; online since September 29, 2016)

Correspondence address

Assist. Prof. Dr. Arif Uzun
Department of Mechanical Engineering
Kastamonu University
Kastamonu, 37150
Turkey
Tel.: +90 366 2802947
Fax: +90 366 2802900
E-mail: auzun@kastamonu.edu.tr

Bibliography
DOI 10.3139/146.111430
Int. J. Mater. Res. (formerly Z. Metallkd.)
107 (2016) 11; page 996 – 1004

ISSN 1862-5282